

## Artificially Induced Reconfiguration of the Vortex Lattice by Arrays of Magnetic Dots

José I. Martín,<sup>1</sup> M. Vélez,<sup>1</sup> A. Hoffmann,<sup>2</sup> Ivan K. Schuller,<sup>2</sup> and J.L. Vicent<sup>1</sup>

<sup>1</sup>*Departamento Física de Materiales, F. Físicas, U. Complutense, 28040 Madrid, Spain*

<sup>2</sup>*Physics Department, University of California–San Diego, La Jolla, California 92093*

(Received 20 January 1999)

Vortex pinning in Nb thin films with rectangular submicrometric magnetic dot arrays exhibits interesting effects. Magnetotransport reveals the existence of two pinning regimes that correspond to two types of resistivity minima with different constant field intervals. The relation with the array lattice parameters indicates that a reconfiguration in the vortex lattice from rectangular to square is induced artificially by the interaction with the dot array. The transition occurs when the elastic energy of the vortex lattice becomes larger than the pinning energy provided by the artificial pinning sites. Using this reconfiguration the pinning energy associated with the magnetic dots can be estimated directly.

PACS numbers: 74.60.Ge

The study of vortex dynamics in type-II superconductors is a challenging field as the phase diagram of the mixed state presents a rich variety of behaviors [1,2]. Interactions between vortices and intrinsic or artificial pinning centers have been the subject of many studies. Random and ordered, artificial pinning centers, such as radiation induced defects [3] or arrays of holes [4] exhibit interesting and unusual effects. In the presence of intrinsic defects, several phase transitions in the vortex lattice of high temperature superconductors are inferred from neutron scattering [5] or transport measurements [6]. These transitions, which occur in a glassy vortex lattice phase, have been interpreted in terms of a balance between the pinning and elastic energy [7,8] of the vortex matter. Also, vortex lattice transformations have been reported in Nb single crystals [9] and, recently, in  $RNi_2B_2C$  compounds ( $R = Y$ , rare earth) [10] due to the coupling to the underlying crystalline symmetry. Therefore, it is interesting to investigate possible transitions in the vortex lattice induced by regular arrays of pinning sites with different symmetries.

Recently, it was shown that vortices in a Nb film can be pinned by periodic arrays of submicrometric magnetic dots fabricated by electron beam lithography [11]. In this case, the flux flow magnetoresistance presents minima at regular field intervals when the vortex lattice geometrically matches the array of dots. This pinning effect was found in several high symmetry configurations such as triangular [11], square [12], or Kagome arrays [13]. To investigate vortex dynamics the elastic properties of the vortex lattice can be probed with low symmetry arrays of pinning centers.

In this work, we have studied the pinning effects of rectangular arrays of magnetic dots. It is found for the first time in a classical low temperature superconductor that the vortex lattice can be artificially distorted into a rectangular configuration by pinning due to a magnetic dot array. As the magnetic field is increased, a transition from a rectangular to a square vortex lattice is observed. These phenomena are analyzed quantitatively using the

balance between vortex pinning and elastic energies and give a direct measure of the pinning energy.

Arrays of circular Ni dots (typical diameter 200 nm and thickness 40 nm) were prepared by electron beam lithography on Si(100) substrates as reported elsewhere [11,14]. The dots were arranged over  $50 \mu\text{m} \times 50 \mu\text{m}$  areas on rectangular ( $c \times d$ ) lattices, with an asymmetry ratio  $f = c/d$  in the range of 1–2.25. A 100 nm thick Nb film was grown on top of the arrays and a  $40 \mu\text{m}$  wide bridge is defined by optical lithography for transport measurements. The superconducting transition temperature of the samples is in the  $T_C = 8\text{--}8.5$  K range. The magnetoresistance curves were measured in a helium cryostat with a 90 kG superconducting magnet. The applied field is perpendicular to the substrate plane, and the transport current is parallel to the long side of the rectangular array unit cell.

The field dependence of the resistivity in the mixed state, for a sample with a rectangular array of dots ( $c \times d = 625 \text{ nm} \times 400 \text{ nm}$ ) is shown in Fig. 1. Several dissipation minima are observed below 1 kG, but the qualitative

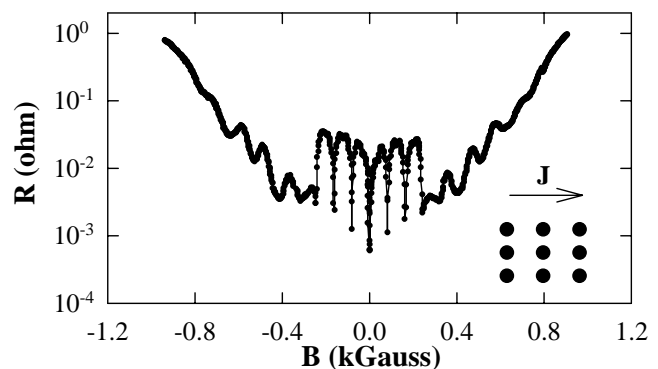


FIG. 1. Field dependence of the resistivity of a Nb film with a rectangular array of Ni dots ( $c \times d = 625 \text{ nm} \times 400 \text{ nm}$ ) measured at  $T = 8.3$  K ( $T_C = 8.5$  K) and  $J = 25 \text{ kA/cm}^2$ . Also shown is a sketch of the current configuration with respect to the dot array.

behavior is quite different from samples with high symmetry dot arrays [11,12]. Two types of minima are clearly present; narrow and deep at low fields, whereas at higher fields (above 300 G) they are broader and shallower. The former type is similar to those observed in Nb films with triangular or square arrays [11,12], while the latter are found only in the present case. A detailed analysis of the minima positions ( $B_n$ ) reveals two regimes characterized by two spacings ( $\Delta B$ ), as shown in Fig. 2(a). At low fields, the interval between two consecutive minima is in excellent agreement with the periodicity derived from the pinning center density  $n_p$ ,  $\Delta B_{\text{theo}}^{\text{rect}} = n_p \Phi_0 = \Phi_0 / cd$ . A comparison between this theoretical value  $\Delta B_{\text{theo}}^{\text{rect}}$  and the experimental  $\Delta B_{\text{low}}$  is given in Table I. This implies that the Ni dots are strong enough pinning centers to distort the vortex lattice into a rectangular configuration to match the underlying array structure. It is worth noting that the rectangular distortion of the vortex lattice to match the dot array is also found for an array (500 nm  $\times$  320 nm) measuring with the current in two different configurations; one along the short side and the other parallel to the long side of the array cell. In the high field range,

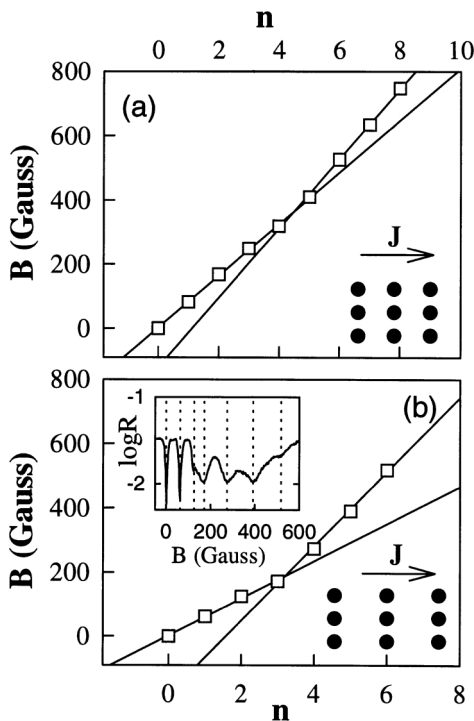


FIG. 2. Position of the minima in resistivity  $B_n$  versus index number  $n$  for Nb films with rectangular arrays of Ni dots of dimensions (a)  $c \times d = 625 \text{ nm} \times 400 \text{ nm}$  and (b)  $c \times d = 900 \text{ nm} \times 400 \text{ nm}$ . Solid lines are linear fits to the data. The index number  $n$  is related in the low magnetic field region to the number of vortices per unit cell of the dot array at the matching condition. The inset shows the field dependence of the resistivity for the Nb sample with a  $900 \text{ nm} \times 400 \text{ nm}$  array at  $T = 7.8 \text{ K}$  ( $T_C = 8.1 \text{ K}$ ) and  $J = 40 \text{ kA/cm}^2$ .

the periodicity  $\Delta B_{\text{high}}$  is much larger and it is similar to the field spacing  $\Delta B = 122 \pm 5 \text{ G}$  found in experiments with (400 nm  $\times$  400 nm) square dot arrays [12]. This suggests that the high field matching peaks are related to the short side (400 nm) of the dot array unit cell, which is also the periodicity of the dot array along the motion direction of the vortex lattice due to the Lorentz force  $\mathbf{F}_L = \mathbf{J} \times \Phi_0$ . Indeed, the theoretically expected matching peak periodicity for a square vortex lattice  $\Delta B_{\text{theo}}^{\text{sq}} = \Phi_0 / d^2 = 129 \pm 5 \text{ G}$  for  $d = 400 \pm 10 \text{ nm}$  is close to the experimentally observed periodicity (see Table I). Thus, at high enough fields, there is a transition in the vortex lattice to a square geometry that is pinned when it matches the short lattice spacing of the Ni array. It is found that the crossover field between these regimes increases as the temperature is reduced and one extra low field minimum is observed below 8.1 K; so that the high field pinning regime becomes favored close to  $T_C$ . The same qualitative behavior is found in a Nb film with a more anisotropic (900 nm  $\times$  400 nm) rectangular array of Ni dots, as shown in Fig. 2(b). Once again  $\Delta B_{\text{low}}$  is in good agreement with the periodicity derived from the Ni dots density while  $\Delta B_{\text{high}}$  corresponds to matching along the short side of the array cell (400 nm) (see Table I). Therefore, the reconfiguration of the vortex lattice from a low field rectangular geometry to a high field square configuration is also observed in this film. The main difference is that in this case the low field range with the sharp minima is smaller than in the previous sample.

The two pinning regimes exhibit a radically different dependence on the applied transport current density. Figure 3 shows several magnetotransport curves measured at the same temperature with different  $J$  values (2.5–100 kA/cm<sup>2</sup>), for a Nb film with a rectangular (625 nm  $\times$  400 nm) array of dots. In the low field regime, the minima are present in a very wide current range starting at the lowest current densities, and only disappearing as the normal state is approached at high currents. On the other hand, the minima found at higher magnetic fields are mainly relevant in the intermediate current range (around  $J = 20 \text{ kA/cm}^2$ ), and disappear for low and high currents. Therefore, the periodic pinning in this second regime is important only at high enough vortex velocities. This

TABLE I. Experimental observed periodicities for the matching peaks at low ( $\Delta B_{\text{low}}$ ) and high ( $\Delta B_{\text{high}}$ ) magnetic fields for two samples with different rectangular dot arrays. For comparison the theoretical periodicities for an exact geometric matching ( $\Delta B_{\text{theo}}^{\text{rect}}$ ) and for a vortex lattice with a square geometry ( $\Delta B_{\text{theo}}^{\text{sq}}$ ) corresponding to the short side of the rectangular array unit cell are indicated.

Lattice $c \text{ (nm)} \times d \text{ (nm)}$	$\Delta B_{\text{low}}$ (G)	$\Delta B_{\text{high}}$ (G)	$\Delta B_{\text{theo}}^{\text{rect}}$ (G)	$\Delta B_{\text{theo}}^{\text{sq}}$ (G)
625 $\times$ 400	$81 \pm 2$	$112 \pm 5$	$83 \pm 2$	$129 \pm 5$
900 $\times$ 400	$58 \pm 3$	$115 \pm 4$	$58 \pm 2$	$129 \pm 5$

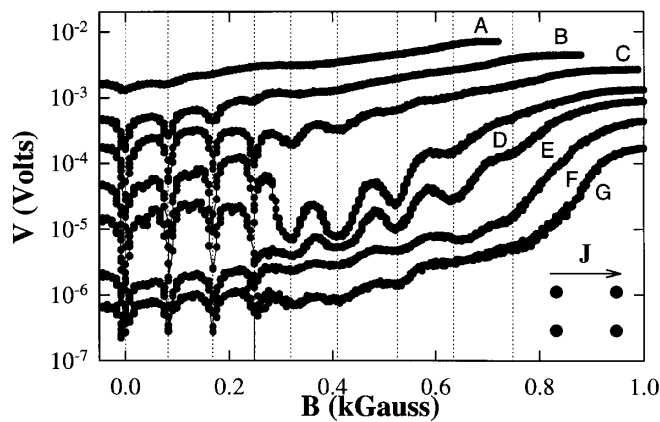


FIG. 3. Field dependence of the longitudinal dissipation of a Nb film with a rectangular array of dots ( $c \times d = 625 \text{ nm} \times 400 \text{ nm}$ ) at  $T = 8.3 \text{ K}$  for different values of the transport current density  $J$ : Curve A,  $100 \text{ kA/cm}^2$ ; curve B,  $62.5 \text{ kA/cm}^2$ ; curve C,  $37.5 \text{ kA/cm}^2$ ; curve D,  $19 \text{ kA/cm}^2$ ; curve E,  $12.5 \text{ kA/cm}^2$ ; curve F,  $6.25 \text{ kA/cm}^2$ ; curve G,  $2.5 \text{ kA/cm}^2$ .

behavior could be related with the competition between the intrinsic random defects of Nb and the synchronized pinning by the dot array, as discussed earlier [11].

The magnetotransport measurements show that rectangular arrays of magnetic dots induce pinning at well defined matching fields, but with very different characteristics from those found with higher symmetry arrays of dots. There are two main features that must be discussed to clarify this new behavior: (i) the presence of two types of minima with different spacing and shape and (ii) the transition between them.

The first low field minima arise due to the deformation of the vortex lattice to a rectangular configuration to match the dot array. Local deformations can be induced in the vortex lattice by random defects to take advantage of the pinning energy. Pinning by random defects creates a very complex strain field on the vortex lattice resulting from the summation of individual pinning forces [1]. On the other hand, artificial regular arrays of pinning centers can induce uniform deformation in the vortex lattice. For instance, in superconducting multilayers with a periodicity in one direction, pinning effects arise over different field ranges depending on the softness of the vortex lattice [15,16]. In our case, at low fields the strong pinning force created by rectangular arrays of magnetic dots produces a global deformation in the vortex lattice, in such a way that the intervortex distance is expanded along one direction and contracted in the perpendicular one, keeping the vortex density constant. This effect gives rise to very sharp minima; pinning at the dots when  $B$  is slightly deviated from the matching condition implies a compression or an expansion in the vortex lattice with a high energy cost. At higher field a reconfiguration to a square lattice occurs because the pinning energy provided by the dot array is not enough to compensate the

elastic energy needed to induce a rectangular configuration in the vortex lattice. So the minima occur when the square vortex lattice matches the dot array along the direction of motion. The broader minima are a result of pinning and consequent matching in one direction only. At fields close to the matching condition, only a shear of the lattice is needed to pin the vortices at the dots, with a lower energy cost than a compression ( $c_{11}$  and  $c_{12}$  are much larger than  $c_{66}$  in the vortex lattice [1]). This explains the different aspects of the matching minima at low and high field. To keep the vortex lattice pinned slightly away from the matching conditions, a lattice compression is involved in the first case, while a shear takes place in the second one.

The transition between both regimes is related to the balance between the pinning and elastic energies. As the magnetic field increases, the extra elastic energy ( $\Delta E_{e1}$ ) stored in the rectangular vortex lattice increases due to enhanced vortex interactions; when this elastic energy becomes larger than the pinning energy ( $\Delta E_P$ ), the rectangular configuration becomes unstable and the vortex lattice reconfigures to a square one. A detailed calculation of this effect would require the determination of the precise vortex lattice arrangement as a function of field. However, as a first approximation, it can be estimated calculating the difference in energy between a rectangular and a square lattice. The Gibbs energy of the vortex lattice can be written as follows [17]:

$$\Delta G = \frac{B}{\Phi_0} \epsilon_1 + \sum_{i>j} F_{ij} - \frac{BH}{4\pi}. \quad (1)$$

The first term is the vortex self-energy; the second corresponds to vortices interactions and is the relevant one to account for the elastic energy associated with the lattice configuration. Its expression is

$$\sum_{i>j} F_{ij} = \frac{\Phi_0^2}{8\pi^2\lambda^2} \sum_{i>j} K_0\left(\frac{r_{ij}}{\lambda}\right), \quad (2)$$

where  $K_0$  is the zeroth-order Hankel function,  $r_{ij}$  is the distance between vortices  $i$  and  $j$ , and  $\lambda$  is the London penetration depth. We have calculated  $\Delta E_{e1}$  using Eq. (2) as  $\Delta E_{e1} = \sum_{i>j} F_{ij}(\text{rectangular}) - \sum_{i>j} F_{ij}(\text{square})$ , considering two lattices with the same vortex density given by the magnetic field. For the calculation, we have taken  $\lambda(T=0) = 90 \text{ nm}$ , which is a typical value for Nb thin films [18];  $\lambda(T) = \lambda(0)/\sqrt{1 - (T/T_C)^4} = 323 \text{ nm}$  at  $T/T_C = 0.98$ , corresponding to the measurement temperature. Vortex interactions in a range of up to  $5000 \text{ nm}$  have been considered to ensure convergence of Eq. (2). Results of these calculations are shown in Fig. 4, for two different asymmetry factors in the dot array and at the values of the matching fields  $B_n$ . The elastic energy clearly increases with the magnetic field, with a higher rate for the more anisotropic sample. Assuming that there is always only one vortex pinned per magnetic dot and that the

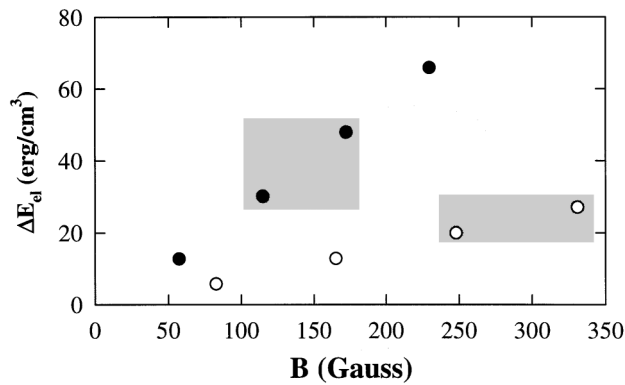


FIG. 4. Field dependence of the elastic energy difference between a square and a rectangular vortex lattice, for different asymmetry ratios:  $f = 2.25 = 900 \text{ nm}/400 \text{ nm}$ , solid circles;  $f = 1.56 = 625 \text{ nm}/400 \text{ nm}$ , open circles. Shadow areas indicate the field, and corresponding energy range, of the reorientation transition defined from the change in shape of the magnetoresistance minima.

interstitial vortices contribution to the pinning energy is negligible the maximum pinning energy is  $\Delta E_P = n_P \epsilon_P$  (where  $\epsilon_P$  is the pinning energy per dot). Thus a crossover from rectangular to square lattice will occur at a field value corresponding to  $\Delta E_P = \Delta E_{el}$ . This condition is met at lower fields for the more anisotropic array, in agreement with the experimental data. From the experimental crossover fields (see shadow areas in Fig. 4), it is possible to estimate the pinning energy per dot as  $\epsilon_P = \Delta E_{el}(\text{crossover})/n_P \approx 10^{-7} \text{ erg/cm}$ . Taking the pinned vortex length as the film thickness  $t = 100 \text{ nm}$ , the vortex pinning energy is  $\epsilon_P \times t = 10^{-12} \text{ erg} \approx 0.6 \text{ eV}$ , which is of the same order of magnitude as for other pinning centers previously studied in classical superconductors [19]. The pinning force derived as  $F_P = (\epsilon_P \times t/\text{dot radius}) \approx 10^{-7} \text{ dyn}$  is of the same order of magnitude as the driving force of the lowest applied currents in Fig. 3. Also, in comparison with recent numerical modelings of vortex dynamics in ordered arrays of defects [20], this pinning energy corresponds to the regime where only two phases are present, either the pinned or the flowing vortex lattice.

In summary, the magnetotransport properties of Nb films with rectangular arrays of magnetic dots have been studied. A transition between two regimes in the vortex lattice is found due to the balance between pinning and elastic energies; at low fields, the pinning force from the dots is strong enough to distort the vortex lattice into a rectangular configuration that matches the dot array. As the field is increased, the elastic energy associated with the lattice becomes dominant and the rectangular distortion becomes unstable, so that vortex lattice is reconfigured to a square geometry. The crossover field between the two regimes is governed by the asymmetry ratio of the Ni dot array.

This work has been supported by the Spanish CICYT (Grant No. MAT96/904), Universidad Complutense, the U.S. National Science Foundation, and the University of California-CLC program. We thank T. Hwa, C. Reichhardt, and G. Zimányi for useful conversations.

- [1] A.M. Campbell and J.E. Evetts, *Adv. Phys.* **21**, 199 (1972).
- [2] G. Blatter, M.V. Feigel'man, V.B. Geshkenbein, A.I. Larkin, and V.M. Vinokur, *Rev. Mod. Phys.* **66**, 1125 (1994).
- [3] L. Civale, A.D. Marwick, T.K. Worthington, M.A. Kirk, J.R. Thompson, L. Krusin-Elbaum, Y. Sun, J.R. Clem, and F. Holtzberg, *Phys. Rev. Lett.* **67**, 648 (1991).
- [4] M. Baert, V.V. Metlushko, R. Jonckheere, V.V. Moshchalkov, and Y. Bruynseraede, *Phys. Rev. Lett.* **74**, 3269 (1995).
- [5] R. Cubitt, E.M. Forgan, G. Yang, S.L. Lee, D. McK. Paul, H.A. Mook, M. Yethiraj, P.H. Kes, T.W. Li, A.A. Menovsky, Z. Tarnawski, and K. Mortensen, *Nature (London)* **365**, 407 (1993).
- [6] R.H. Koch, V. Foglietti, W.J. Gallagher, G. Koren, A. Gupta, and M.P.A. Fisher, *Phys. Rev. Lett.* **63**, 1511 (1989).
- [7] K. Moon, R.T. Scalettar, and G.T. Zimányi, *Phys. Rev. Lett.* **77**, 2778 (1996).
- [8] S. Ryu, A. Kapitulnik, and S. Doniach, *Phys. Rev. Lett.* **77**, 2300 (1996).
- [9] D.K. Christen, H.R. Kerchner, S.T. Sekula, and P. Thorel, *Phys. Rev. B* **21**, 102 (1980).
- [10] M.R. Eskildsen, P.L. Gammel, B.P. Barber, A.P. Ramirez, D.J. Bishop, N.H. Andersen, K. Mortensen, C.A. Bolle, C.M. Lieber, and P.C. Canfield, *Phys. Rev. Lett.* **79**, 487 (1997).
- [11] J.I. Martín, M. Vélez, J. Nogués, and I.K. Schuller, *Phys. Rev. Lett.* **79**, 1929 (1997).
- [12] Y. Jaccard, J.I. Martín, M.C. Cyrille, M. Vélez, J.L. Vicent, and I.K. Schuller, *Phys. Rev. B* **58**, 8232 (1998).
- [13] D.J. Morgan and J.B. Ketterson, *Phys. Rev. Lett.* **80**, 3614 (1998).
- [14] J.I. Martín, Y. Jaccard, A. Hoffmann, J. Nogués, J.M. George, J.L. Vicent, and I.K. Schuller, *J. Appl. Phys.* **84**, 411 (1998).
- [15] H. Raffy, J.C. Renard, and E. Guyon, *Solid State Commun.* **11**, 1679 (1972).
- [16] M. Vélez, J.I. Martín, and J.L. Vicent, *Appl. Phys. Lett.* **67**, 3186 (1995).
- [17] M. Tinkham, *Introduction to Superconductivity* (McGraw-Hill, New York, 1996), p. 156.
- [18] R.F. Broom, *J. Appl. Phys.* **47**, 5432 (1976); H. Zhang, J.W. Lynn, C.F. Majkrzak, S.K. Satija, J.H. Kang, and X.D. Wu, *Phys. Rev. B* **52**, 10395 (1995).
- [19] M.R. Beasley, R. Labusch, and W.W. Webb, *Phys. Rev.* **181**, 682 (1969).
- [20] C. Reichhardt, C.J. Olson, and F. Nori, *Phys. Rev. B* **58**, 6534 (1998).